WIP is essential for lytic granule polarization and NK cell cytotoxicity

Konrad Krzewski, Xi Chen, and Jack L. Strominger*

Department of Molecular and Cellular Biology, Harvard University, 7 Divinity Avenue, Cambridge, MA 02138

Contributed by Jack L. Strominger, December 9, 2007 (sent for review December 7, 2007)

Natural killer (NK) cells play important roles in host immunity by killing virus-infected and tumor cells. Killing of the target cell is achieved by formation of an immune synapse and localized secretion of lytic granules containing perforin and granzymes. Here, we demonstrate that Wiskott–Aldrich syndrome protein (WASp)-interacting protein (WIP), important in generation of a large complex of proteins involved in actin cytoskeleton rearrangements, is indispensable for NK cell cytotoxicity. WIP knockdown completely inhibited cytotoxicity, whereas overexpression of WIP enhanced NK cell cytolytic ability. WIP was found to colocalize with lytic granules. WIP segregated to the lysosomal fraction, where granzyme B activity was also found, and the interaction between WIP and granules was independent of WASp. Importantly, WIP knockdown inhibited polarization of lytic granules to the immune synapse, but not conjugate formation. These results indicate that WIP is involved in lytic granule transport and is essential for regulation of NK cell cytotoxic function.

WASp | perforin | granzymes | immune synapse | NK cytolytic activity

Natural killer (NK) cells form a relatively small subset of lymphocytes. Still, they play very important roles in immunosurveillance of cancer or virus-infected cells and contribute to antigen-specific immune response through production of chemokines and cytokines, such as IFN-γ (1, 2).

NK cell activity is regulated by a variety of activating or inhibitory receptors. Interaction of inhibitory receptors with their ligands negatively regulates NK cell activity. Conversely, activation of NK cells, mediated by recognition of their ligands by activation receptors, triggers a complex and highly regulated response leading to death of a target cell (3–5). Killing is achieved by localized secretion of lytic granules containing granzymes and perforin at the cell–cell contact site, known as the immune synapse (6, 7). Perforin forms pores in the cell membrane, allowing granzymes to enter the target cell. Granzymes belong to the serine protease family and induce the death of target cells through caspase-dependent activation of apoptosis or in a caspase-independent manner by SET complex-mediated induction of single-strand DNA nicks (8).

Virtually all cytolytic responses require actin cytoskeleton rearrangements for proper cell adhesion, immune synapse formation, sustained signaling, and delivery of lytic granules to the target cell (9–11). Actin polymerization at the leading edge of the cell is facilitated by Wiskott–Aldrich syndrome protein (WASp)-mediated activation of the Arp2/3 complex (12). Because WASp is a key regulatory protein of Arp2/3 activity and thus actin polymerization, its activity is tightly controlled by a variety of adaptor and regulatory proteins, including the WASp-interacting protein (WIP) (13, 14).

Recent reports provide evidence for a role of WIP as a new factor important for lymphocyte activity. Originally identified as WASp binding protein (15), WIP was later demonstrated to actively participate in actin rearrangements through retardation of WASp-mediated (16) and enhancement of cortactin-mediated actin polymerization (17). WIP binds and stabilizes filamentous actin (F-actin) (16), is required for generation of a large complex of proteins involved in actin cytoskeleton rearrangements (18) and is important for creation of membrane protrusions (16, 19). Moreover, WIP plays an important role in activation of T, B, and mast cells (20, 21). Despite WIP involvement in variety of processes, the exact mechanism of WIP function remains to be elucidated.

Here, we show that WIP associates with lytic granules in NK cells. Disruption of WIP expression by RNAi surprisingly did not affect cell adhesion and conjugation, but severely impaired lytic granule polarization to the immune synapse, resulting in inhibition of NK cell cytotoxic activity. The identification of WIP involvement in lytic granule transport provides insight into comprehending the multiplicity of WIP functions in regulation of NK cell activity.

Results and Discussion

WIP Colocalizes with Lytic Granules in NK Cells. We have shown that, in response to NK cell stimulation, WIP polarized toward the immune synapse and accumulated in the area adjacent to the immune synapse (18). Although the exact role of WIP in that process was not clear, WIP distribution was similar to that observed for lytic granules. Therefore, the cellular localization of WIP and lytic granules was examined in YTS cells expressing FLAG-tagged WIP.

Analysis of staining of FLAG-WIP and perforin, a marker for lytic granules, showed that WIP colocalized with the majority of perforin in both resting and activated YTS cells. In resting cells 71 $\pm$ 11% of FLAG-WIP colocalized with perforin and 74 $\pm$ 17% of perforin colocalized with FLAG-WIP. Although FLAG-WIP and perforin were dispersed in the cytoplasm of resting cells, activation of NK cells by mixing with susceptible target cells resulted in translocation and polarization of both WIP and perforin toward the immune synapse. However, the colocalization percentages did not change significantly after activation of NK cells (76 $\pm$ 7% of WIP with perforin and 78 $\pm$ 9% of perforin with WIP) (Fig. 1*A*).

A large pool of endogenous WIP also colocalized with perforin [see supporting information (SI) Fig. 5*A*], validating the result observed for FLAG-WIP; however, the binding of polyclonal anti-WIP antibodies was characterized by a relatively high background (SI Fig. 5; data not shown). Because nonspecific interactions of these antibodies could not be excluded, the rest of the study was performed by using FLAG-WIP.

The observed colocalization of WIP and perforin indicated the possible association of WIP and lytic granules. To test this hypothesis, the lysosomal fraction from YTS cells was isolated, using the fact that lytic granules have characteristics of secretory lysosomes (22). The fractionation of cell compartments and separation of lysosomal fraction on an Iodoxanol density gradi-

Author contributions: K.K. designed research; K.K. and X.C. performed research; K.K. and X.C. contributed new reagents/analytic tools; K.K. analyzed data; and K.K. and J.L.S. wrote the paper.

The authors declare no conflict of interest.

*To whom correspondence should be addressed. E-mail: jlstrom@fas.harvard.edu.

This article contains supporting information online at www.pnas.org/cgi/content/full/0711593105/DC1.

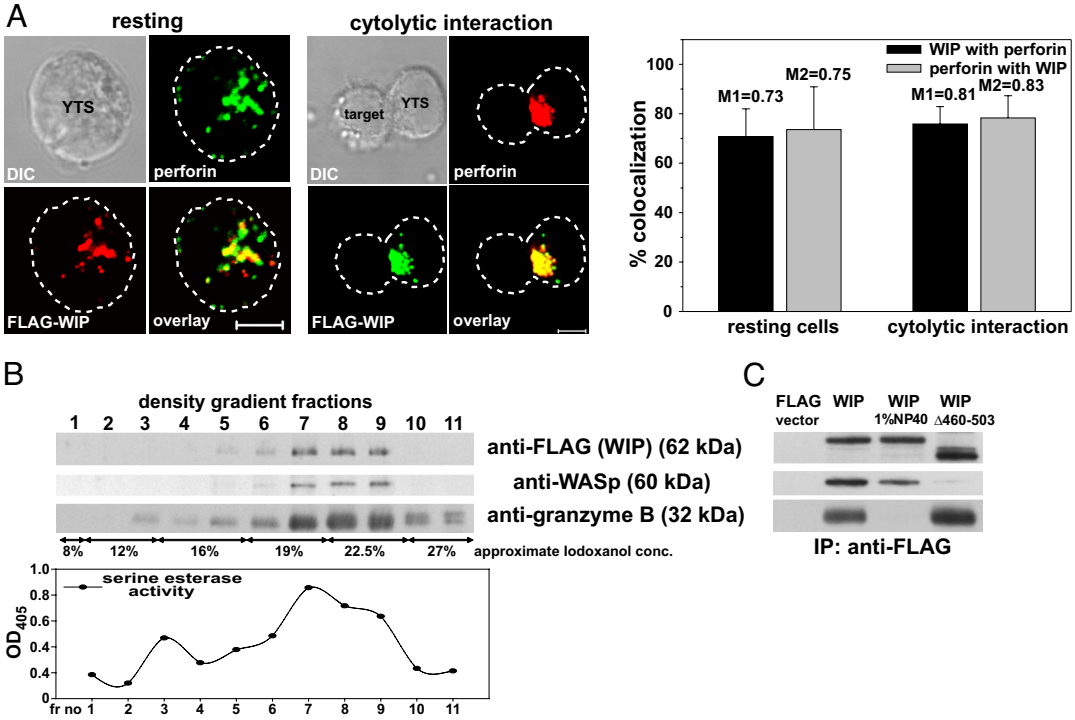

Fig. 1. WIP is associated with lytic granules in NK cells. (*A*) Colocalization of FLAG-WIP and perforin in resting (*Left*) and activated (*Center*) YTS cells. YTS cells expressing FLAG-WIP, unconjugated or conjugated by mixing for 10 min at 37°C with 721.221 target cells, were stained with Cy3-conjugated anti-FLAG mAb (red) and AlexaFluor 647-conjugated anti-perforin (green) antibodies. (Scale bar: 5 μm.) The graph (*Right*) displays the percentage of FLAG-WIP colocalizing with perforin (black bars) and perforin that colocalized with FLAG-WIP (gray bars) in either resting or activated NK cells ($n \geq 10$). Values above each bar represent Manders' colocalization coefficients. Error bars represent SD. (*B*) WIP and WASp are found in the lysosomal fraction of NK cells. YTS cells expressing FLAG-WIP were homogenized and fractionated by centrifugation, and crude lysosomal fraction was resolved on an 8–27% Iodoxanol density gradient. Proteins from gradient fractions were resolved on a NuPage gel, transferred to a PVDF membrane, and subsequently immunobloted with anti-FLAG, anti-WASp, and anti-granzyme B antibodies. The serine esterase activity (a marker for granzyme activity) was determined in each density gradient fraction and displayed graphically below. (*C*) WIP association with lytic granules is independent of WASp and requires intact granules. YTS cells, transfected with either FLAG-WIP or FLAG-WIPΔ460–503 or FLAG expression vector alone, were lysed by homogenization. Crude lysosomal fractions either nontreated or treated with 1% Nonidet P-40 (to solubilize cell membranes) were immunoprecipitated with anti-FLAG mAb. Immunoprecipitated proteins were resolved on a NuPage gel, transferred to a PVDF membrane, and immunobloted with anti-FLAG, anti-WASp, and anti-granzyme B antibodies. The molecular masses of the proteins, relative to masses of molecular markers, are shown in parentheses.

ent revealed that WIP was present in the fractions containing granzyme B, a vital component of lytic granules of cytotoxic lymphocytes, as determined by immunoblotting and serine esterase activity, a marker for granzyme B activity (Fig. 1*B*).

A WIP binding partner, WASp, was also present in the same fractions (Fig. 1*B*). Because WASp was found on the surface of both endocytic and exocytic vesicles (23, 24) and could therefore provide a docking site for WIP, the ability of WIP to associate with lytic granules without WASp was investigated. Immunoprecipitation with wild-type FLAG-WIP showed that WIP was able to coimmunoprecipitate granzyme B and WASp, verifying the result obtained from density gradient fractionation. Most importantly, a WIP mutant with deletion of the WASp binding domain, FLAG-WIPΔ460–503 (18), was still able to pull down granzyme B even though its WASp binding ability was lost (Fig. 1*C*). Thus, WIP associates with lytic granules in NK cells and this interaction is independent of WASp.

Interestingly, destruction of vesicle integrity with 1% Nonidet P-40 resulted in the inability of WIP (Fig. 1*C*) or WIPΔ460–503 (data not shown) to pull down granzyme B, indicating that the interaction of WIP with lytic granules required intact granules and WIP resided on the surface of the granules. It is not yet clear whether WIP binding to granules is direct or indirect. WIP does not contain any domains that directly bind lipids, but secretory granules contain a variety of proteins on their surface, including WIP binding partners such as actin, myosins, or PKC family proteins (25) and, thus, the interaction could be indirect. Additionally, WIP is a proline-rich protein, capable of binding SH3 domain-containing proteins and its association with lytic granules may be mediated by more complex interactions through adaptor proteins as well.

WIP Knockdown Inhibits NK Cell Cytotoxicity Without Affecting Conjugate Formation. WIP has been shown to be involved in NK cell cytotoxicity. WIP knockdown in the NK tumor cell line YTS impaired its ability to lyse target cells (18), although the mechanism underlying this phenomenon has not been elucidated. Assessment of YTS cytotoxicity was repeated and expanded by the analysis of the effects of WIP overexpression in YTS cells and WIP knockdown in pNK cells. WIP knockdown in YTS cells and, importantly, also in pNK cells resulted in almost complete inhibition of cytotoxicity (Fig. 2*A*). Interestingly, WIP overexpression enhanced cytotoxicity of YTS cells ≈30–40%, when compared with untransfected or control-transfected cells. Thus, WIP is a crucial component of the NK cell cytotoxic machinery.

Because WIP plays a role in extension of cell protrusions important for cell adhesion (19, 20), the influence of WIP knockdown on cell–cell conjugate formation was investigated next. Flow cytometry analysis of conjugates formed between NK cells and target cells did not reveal any substantial change in the fraction of conjugates formed by using untransfected (38 ± 4%) or vector-transfected (46 ± 6% for FLAG vector and 41 ± 7%

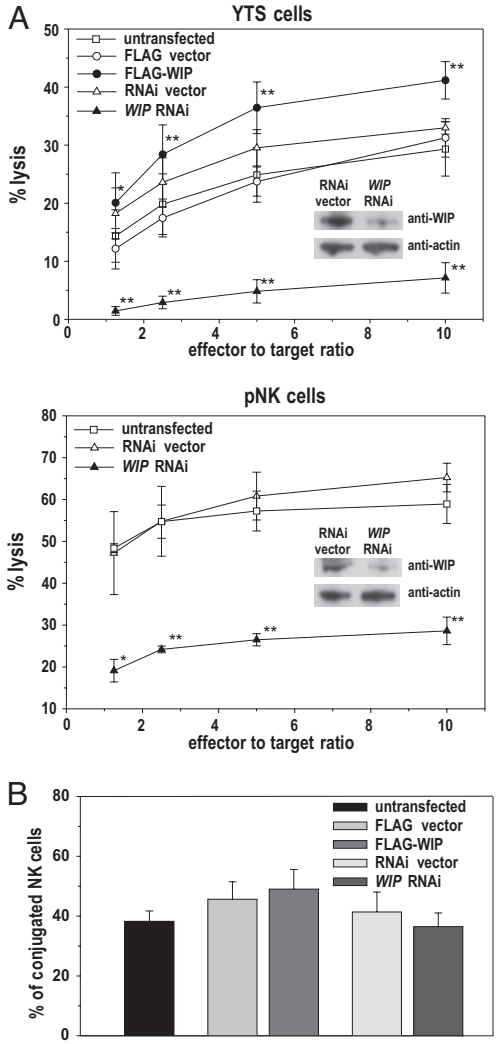

Fig. 2. WIP knockdown inhibits NK cell cytotoxicity despite normal conjugate formation. (*A*) Cytolytic activity of YTS (*Upper*) and pNK (*Lower*) cells, untransfected or transfected with either FLAG-WIP (YTS only) or *WIP* RNAi. Cells transfected with FLAG expression vector (FLAG; YTS only) or empty RNAi vector (RNAi vector) were used as additional controls. (*Insets*) Western blots show decrease of WIP expression due to WIP knockdown, with anti-actin immunostaining as a loading control. The percentage of 721.221 target cell lysis for different effector-to-target ratio is shown. Error bars represent SD. The values are based on five and three separate experiments for YTS and pNK cells, respectively. The asterisks indicate statistical significance (*, $P < 0.05$; **, $P < 0.01$ by Student's *t* test) when compared with control-transfected cells. (*B*) YTS cells, untransfected or transfected with either *WIP* RNAi, empty RNAi vector (RNAi vector), FLAG expression vector (FLAG), or with FLAG-WIP, were stained with CD56-APC antibodies and mixed with RFP-expressing 721.221 target cells. Cells were allowed to form conjugates for 30 min at 37°C, fixed, and analyzed by flow cytometry. The graphs represent the population of YTS cells conjugated with target cells, as determined by the measurement of the percentage of $CD56^+RFP^+$ double-positive cells from the total pool of live $CD56^+$ cells.

for RNAi vector) YTS NK cells, compared with the cells with RNAi-disrupted WIP expression (36 ± 5%) (Fig. 2*B*). The YTS cells overexpressing WIP displayed the most efficient conjugate formation (49 ± 7%), but the difference was not statistically significant. Thus, *WIP* RNAi-induced inhibition of NK cell cytotoxicity is not mediated by the decrease of cell–cell adhesion.

WIP Knockdown Prevents Lytic Granule Polarization to the Immune Synapse. The observation that WIP was associated with lytic granules and was not involved in regulation of cell adhesion raised the question whether the inhibition of NK cell cytotoxicity by *WIP* RNAi could be due to WIP interaction with lytic granules. It has been shown that, after NK cell activation, WIP translocated to the immune synapse area. However, only a marginal portion of WIP localized with the actin cytoskeleton within the synaptic region. The majority of WIP was found in the region adjacent to the immune synapse, but the role of its accumulation was not clear (see Fig. 4 and figure S1 in ref. 18). Therefore, the effects of WIP knockdown on granule polarization were examined.

After conjugation with 721.221 target cells, resulting in NK cell activation, the majority of YTS (75 ± 5%) and pNK (72 ± 4%) cells polarized perforin-containing lytic granules toward the immune synapse. However, WIP knockdown resulted in a dramatic decrease of perforin movement toward the immune synapse: only 35 ± 2% of YTS and 36 ± 6% of pNK cells displayed perforin polarization (Fig. 3). The defects in extent of polarization were confined mostly to lytic granule translocation, because the extent of F-actin polarization, a vital component of the immune synapse (10, 26), did not appear to be affected either in YTS or in pNK cells. F-actin accumulation at the immune synapse in *WIP* RNAi-treated cells was virtually the same as in untransfected cells (86 ± 8% vs. 82 ± 2% in YTS cells and 78 ± 5% vs. 71 ± 6% in pNK cells) (Fig. 3). This finding was surprising in view of reports demonstrating the ability of WIP to stabilize F-actin *in vitro* (16) and the disruptive effects of WIP knockout on the amount and distribution of F-actin at the cell periphery in T and B cells (20). However, it was possible that accumulation of F-actin from the target cell at the immune synapse masked changes in F-actin content in NK cells. To address that issue, F-actin accumulation in NK cells was assessed by using anti-LFA-1-coated beads to cross-link LFA-1 on the surface of NK cells, an approach shown to be successful in inducing actin polymerization at the cell–bead interface (27). Analysis of F-actin accumulation at the interface between NK cell and polystyrene bead revealed no dramatic change in F-actin polarization (Fig. 4*A*). F-actin still accumulated at the bead–cell contact area in cells with WIP knockdown. However, the amount of accumulated F-actin was somewhat decreased in *WIP* RNAi cells. Additionally, overexpression of WIP appeared to slightly enhance the amount of F-actin accumulated at the cell–bead contact area (Fig. 4*A*). Furthermore, analysis of F-actin accumulation at the immune synapse revealed that cells with RNAi-disrupted WIP expression tended to form smaller conjugates (58 ± 12 μm^2 in *WIP* RNAi cells vs. 77 ± 23 μm^2 in untransfected cells) (Fig. 4*B*). However, because the conjugate area depends on multiple factors (e.g., duration of conjugation, strength of the activation signal, size of the cell, etc.), this result is open to interpretation. Nevertheless, the lack of drastic changes in the accumulation of F-actin at the immune synapse in *WIP* RNAi-treated NK cells indicated that WIP is not critical for the early stages in synapse formation. Alternatively, the remaining low level of expression of WIP in *WIP* RNAi cells (Fig. 2*A Inset*) might have been sufficient to stabilize F-actin structures. Vector alone did not affect polarization of the studied molecules, because cells transfected with RNAi vector were indistinguishable from untransfected cells (Fig. 3 *A* and *B Middle*). YTS cells overexpressing FLAG-WIP and cells transfected with FLAG alone displayed identical patterns of polarization of F-actin and perforin as untransfected cells (data not shown).

WIP appears to play an important role in lytic granule movement toward the immune synapse in activated NK cells, providing at least a partial explanation for the observed inhibition of cytotoxicity in WIP-deficient cells. The cells with WIP expression disrupted by RNAi formed conjugates with target cells similarly to normal NK cells (Fig. 2*B*), indicating that the decrease in NK cell cytotoxicity was not due to impaired cell–cell adhesion, but rather to decreased lytic granule polarization to

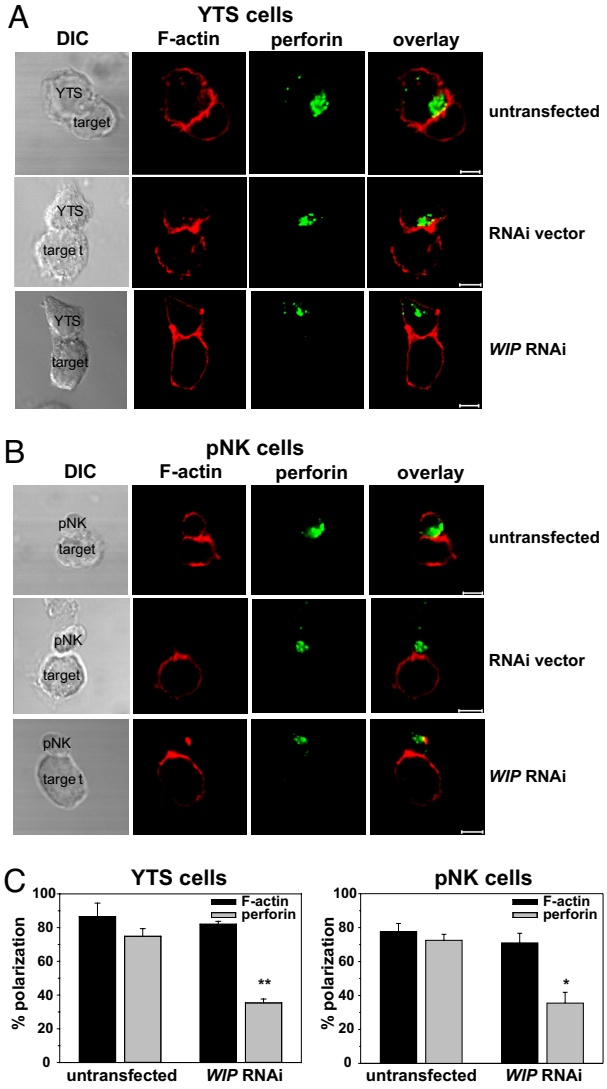

Fig. 3. Knockdown of WIP prevents granule but not F-actin polarization to the immune synapse in NK cells. YTS (*A*) and pNK (*B*) cells, untransfected (*Top*) or transfected with empty RNAi vector (*Middle*) or *WIP* RNAi (*Bottom*), were activated by mixing with 721.221 target cells for 15 min at 37°C. Cells were next stained with AlexaFluor 568-conjugated phalloidin (red) and AlexaFluor 647-conjugated anti-perforin antibodies (green) to visualize F-actin and lytic granules, respectively. (Scale bar: 5 μm.) (*C*) The percentages of F-actin and perforin polarization toward the cell–cell contact site (immune synapse) in YTS (*Left*) and pNK (*Right*) cells conjugated with 721.221 target cells. Error bars represent SD. The values were determined by evaluation of 100–200 conjugates in two to four separate experiments. The asterisks indicate statistical significance (*, $P < 0.05$; **, $P < 0.01$ by Student's *t* test) when compared with control.

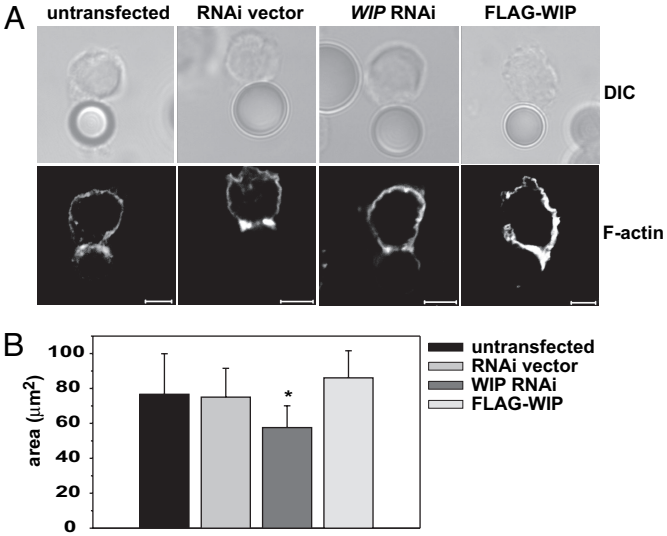

Fig. 4. WIP knockdown does not prevent F-actin polarization, but affects the area of F-actin accumulation at the cell–cell interface. (*A*) F-actin accumulation at the cell–bead interface. YTS cells either untransfected or transfected with empty RNAi vector, *WIP* RNAi, or FLAG-WIP were mixed with anti-LFA1 mAb-coated polystyrene beads for 60 min at 37°C. The cells were then stained with AlexaFluor 568-conjugated phalloidin to visualize F-actin. (Scale bar: 5 μm.) (*B*) The area of F-actin accumulated at the cell–cell contact site. Untransfected YTS cells or YTS cells transfected with empty RNAi vector, *WIP* RNAi, or FLAG-WIP were mixed with 721.221 target cells 10 min at 37°C, followed by staining with AlexaFluor 568-conjugated phalloidin and AlexaFluor 647-conjugated anti-perforin antibodies (to distinguish NK cells from target cells). F-actin at the immune synapse was visualized by taking a series of images of conjugated cells in the *z* plane, from which the area of F-actin accumulation was measured. $n \geq 14$. Error bars represent SD. The asterisk indicates statistical significance ($P < 0.05$ by Student's *t* test) when compared with control.

the immune synapse. It is noteworthy that even though the inhibition of perforin polarization was not complete, knockdown of WIP abolished NK cell cytotoxicity (Fig. 2*A*). It is possible, that WIP knockdown could affect cell activity at different levels. For example, WIP has been shown to influence WASp stability and expression levels in T cells (28, 29). Indeed, knockdown or overexpression of WIP also affected WASp levels in NK cells (see SI Fig. 5*B*), confirming the widespread nature of this phenomenon and providing an additional mechanism for regulation of NK cell activity. Because WASp is important for the immune synapse dynamics (26, 30), the decrease in WASp levels after WIP knockdown could contribute to changes in the immune synapse stability and, therefore, impaired cytotoxicity. Moreover, even though actin polarization and accumulation at the synapse in *WIP*-RNAi cells was not strongly affected, some alterations were apparent and the contribution of WIP to actin dynamics in NK cells is not ruled out. Thus, the decrease in cytotoxicity in *WIP* RNAi cells could be due to cumulative defects caused by disruption of WIP expression (e.g., WASp degradation, destabilization of the F-actin network, and inhibition of granule polarization). It is therefore important to investigate next whether disruption of WIP expression could affect additional processes in the cell, for example, microtubule-organizing center (MTOC) polarization.

The exact function of WIP has not yet been fully defined. Initially, a WASp binding protein (15) involved in stabilization of WASp (28, 29) and regulation of its activity (16), WIP was further demonstrated to have other functions, such as involvement in actin polymerization (16, 17), cell protrusion formation (19, 20), and endocytosis (31, 32). WIP has also been demonstrated to be essential for formation of a large complex of proteins involved in actin cytoskeleton rearrangements in response to NK cell activation. This complex, composed of WIP, WASp, actin, and myosin IIA, formed and translocated to the immune synapse area in response to NK cell activation, whereas inhibitory signaling affected complex formation and prevented its polarization to the cell–cell contact site, indicating its importance in NK cell cytotoxicity (18). The finding that WIP colocalizes with lytic granules, pulls down granzyme B (Fig. 1) (together with other components of multiprotein complex; data not shown), and is critical for both perforin (Fig. 3) and multiprotein complex polarization (18) to the immune synapse, indicates that the large structure could be involved in lytic

granule transport. Lytic granules are initially moved along microtubules. However, it is not yet fully understood whether they are transported only by using the MTOC-derived microtubule set or by using, in addition, a recently described second set originating in the Golgi and extending toward the cell periphery (33), or both. Nevertheless, lytic granule delivery and exocytosis at the immune synapse area may require translocation to the actin cytoskeleton network. Even though the MTOC in activated cytotoxic lymphocytes is positioned very close to the cell membrane, there are no microtubules at the immune synapse itself (34), and most likely the granules have to be transferred to the actin cytoskeleton to be secreted. In this regard, the Arp2/3 complex found at the immune synapse was proposed to be involved in driving granules to the plasma membrane (35), and the knockdown of the actin motor protein myosin IIA prevented exocytosis of polarized granules (36). WIP with its ability to bind F-actin and form a complex of proteins involved in actin rearrangements (i.e., WASp and myosin IIA) could act as a link between granules and the actin cytoskeleton. Thus, WIP plays important functions at many levels in NK cell activity and our understanding of its role is quickly evolving from an adaptor to a protein crucial for lymphocyte activity.

Materials and Methods

Antibodies and Reagents. The following antibodies were used: anti-FLAG (clone M2; Sigma-Aldrich), anti-WASP (US Biological), anti-granzyme B (Sigma-Aldrich), anti-WIP (Santa Cruz Biotechnology), anti-perforin (clone dG9; AlexaFluor 647-conjugated; BioLegend), anti-actin (Sigma-Aldrich), anti-rabbit IgG (clone RG-96, HRP-conjugated; Sigma-Aldrich), anti-CD56 (APC-conjugated; BD Biosciences), anti-LFA-1 (clone TS1/18; gift from T. Springer, Boston). Phalloidin (AlexaFluor 568-conjugated) and NuPage reagents were from Invitrogen. All other chemicals were from Sigma-Aldrich, unless stated otherwise.

Cells and Transfectants. B lymphoblastoid cell line 721.221 and the human NK tumor cell line YTS expressing FLAG-WIP and FLAG-WIPΔ460-503 were cultured as described in ref. 18. Human pNK cells were isolated and grown as described in ref. 26.

Generation of the RFP-221 Cells. pDsRed2-C1 plasmid (Clontech) was electrotransfected into 721.221 cells by using Nucleofector I (Amaxa Biosystems). The RFP-positive cells were sorted by using MoFlo High Performance Cell Sorter (DakoCytomation) and cultured in RPMI medium supplemented with G418 (1.6 mg/ml).

WIP RNAi. Vector-based RNAi targeting the 5′-GGAGGTTTCCTGTGCCTTCT-3′ sequence in *WIP* cDNA, used to knockdown WIP expression in YTS cells was described in ref. 18.

For lentiviral-based delivery of RNAi into pNK cells, the construct targeting the 5′-GGGTGGGAATCGGTAAGAAAT-3′ segment in the *WIP* 3′ UTR region was inserted between the ClaI and EcoRI sites of the pLKO.3GFP vector (gift from D. Mathis, Boston). The resulting plasmid construct was sequenced to confirm the correct sequence.

Lentivirus Infection of Human pNK Cells. pLKO.3GFP-WIP constructs, together with the pHR-CMV-8.2deltaVpR and pHR-CMV-VSVG helper constructs (gifts from D. Trono, Lausanne, Switzerland), were transfected into 293T cells by using Fugene 6. The lentivirus-containing medium was then added to 1×10^7 NK cells. The infection was carried out for 10 h in the presence of 8 μg/ml polybrene. After 48 h, GFP-positive pNK cells were sorted by using the MoFlo Cell Sorter and subsequently cultured in MyeloCult media.

Isolation of Lytic Granules. The lysosomal fraction containing lytic granules was isolated from YTS cells by using a Lysosomal Isolation Kit, according to manufacturer's instructions. Half-milliliter fractions were collected. For the immunoblotting analysis, the gradient fractions samples were resolved on a 4–12% NuPage gels, transferred to PVDF membrane and analyzed as described below. For the serine esterase assay, 50 μl of each fraction were placed in a well of a 96-well plate, followed by addition of 50 μl of 1 mM 5,5′-dithio-bis(2-nitrobenzoic acid) and 25 μl of 0.5 mM Na-benzyloxycarbonyl-L-lysine thiobenzyl ester. The reaction was stopped by addition of 1 mM PMSF, and the absorbance values at 405 nm were measured with MRX Microplate Reader (Dynex Technologies).

Immunoprecipitation and Western Blotting. Gently homogenized in a Dounce homogenizer were 1×10^8 cells. The homogenized cells were centrifuged at $1{,}000 \times g$ for 10 min at 4°C to remove nuclear debris. Next, the collected supernatant was centrifuged at $20{,}000 \times g$ for 20 min at 4°C to pellet a crude lysosomal fraction, and the pellet was resuspended in 1 ml of ice-cold Extraction Buffer from the Lysosomal Isolation Kit. The lysosomal fraction from YTS cells expressing FLAG-WIP was divided into two tubes. Nonidet P-40 was added to one tube to the final concentration of 1% and the second tube was left untreated. YTS/FLAG cells, used as a control, were also treated with 1% Nonidet P-40. The lysosomal fractions were immunoprecipitated overnight with anti-FLAG antibody coupled to protein G agarose beads. Immunoprecipitated proteins were immunoblotted with anti-FLAG, anti-WASp, or anti-granzyme B antibodies, by using standard procedures. Immunoblots were developed by using ECL Western Blotting Detection Reagents (Amersham Biosciences).

^{51}Cr Release Assay. NK cell cytotoxicity was evaluated by ^{51}Cr release assay as described in ref. 18.

Cell Conjugation Assay. NK cells (5×10^5) were stained with APC-conjugated CD56 mAb, and washed and mixed with RFP-expressing 721.221 target cells at 1:1 ratio. Cells were immediately transferred to 37°C and incubated for 20 min, followed by fixation with 0.5% paraformaldehyde. Next, cells were analyzed with a FACSCalibur flow cytometer (Becton Dickinson). The conjugate percentages were established in four separate experiments by determination of CD56+ RFP+ double-positive cells, representing NK cells conjugated with target cells, from the total pool of live CD56+ NK cells.

Microscopy. The cells were fixed and stained with AlexaFluor 647-conjugated anti-perforin monoclonal antibodies, followed by either Cy3-cojnugated anti-FLAG monoclonal antibodies or AlexaFluor 568-conjugated phalloidin. In endogenous WIP staining, cells were first stained with AlexaFluor 647-conjugated anti-perforin mAb, followed by staining with anti-WIP polyclonal antibody and AlexaFluor 488-conjugated donkey anti-goat secondary antibody. The LFA-1 cross-linking was performed essentially as described in ref. 27, with the exception that biotinylated anti-CD18 mAb were first coated on 7.4-μm polystyrene beads (Spherotech) and then added to the cells, followed by cell fixation and staining with AlexaFluor 568-conjugated phalloidin. Cell conjugates, mounted in ProLong Gold medium (Invitrogen) were visualized by a Zeiss LSM 510 Axiovert 100M laser-scanning confocal microscope at room temperature. The images were obtained by using 63× Zeiss Plan-Apochromat objective and LSM510 v3.2 software. Images shown represent a single optical section, unless stated otherwise. Scale bars in all images represent 5 μm. The percentage values for conjugated cells were determined by evaluation of 100–200 conjugates in randomly selected fields, in two to four separate experiments. Contact areas were calculated by scanning ≥14 cell conjugates in the *z* plane, to visualize the entire interface between the NK and target cell, followed by measurement of total area occupied by F-actin at the cell–cell contact point, by using LSM510 v3.2 software. FLAG-WIP and perforin colocalization were assessed by analysis of at least 10 images and measurement of voxels occupied by two fluorophores by using BioImage Arbor XD v0.9 software (University of Jyväskylä and University of Turku, Finland) (37). The colocalization threshold values were calculated automatically by BioImage Arbor software, as recommended in ref. 38.

Supporting Information. SI Fig. 5 shows the localization of endogenous WIP and perforin in resting and activated YTS cells (SI Fig. 5*A*) and changes in WASp expression level in different WIP transfectants (SI Fig. 5*B*).

ACKNOWLEDGMENTS. This work was supported by National Institutes of Health Grant AI49524.

1. Biron CA, Nguyen KB, Pien GC, Cousens LP, Salazar-Mather TP (1999) Natural killer cells in antiviral defense: function and regulation by innate cytokines. *Annu Rev Immunol* 17:189–220.
2. Cerwenka A, Lanier LL (2001) Natural killer cells, viruses and cancer. *Nature Rev* 1:41–49.
3. Blery M, Olcese L, Vivier E (2000) Early signaling via inhibitory and activating NK receptors. *Hum Immunol* 61:51–64.
4. Lanier LL (2003) Natural killer cell receptor signaling. *Curr Opin Immunol* 15:308–314.
5. Vivier E, Nunes JA, Vely F (2004) Natural killer cell signaling pathways. *Science* 306:1517–1519.

6. Berke G (1997) Killing mechanisms of cytotoxic lymphocytes. *Curr Opin Hematol* 4:32–40.
7. Trambas CM, Griffiths GM (2003) Delivering the kiss of death. *Nature Immunol* 4:399–403.
8. Voskoboinik I, Smyth MJ, Trapani JA (2006) Perforin-mediated target-cell death and immune homeostasis. *Nature Rev* 6:940–952.
9. Billadeau DD, Nolz JC, Gomez TS (2007) Regulation of T-cell activation by the cytoskeleton. *Nature Rev* 7:131–143.
10. Carpen O, Virtanen I, Lehto VP, Saksela E (1983) Polarization of NK cell cytoskeleton upon conjugation with sensitive target cells. *J Immunol* 131:2695–2698.
11. Vyas YM, Maniar H, Dupont B (2002) Visualization of signaling pathways and cortical cytoskeleton in cytolytic and noncytolytic natural killer cell immune synapses. *Immunol Rev* 189:161–178.
12. Machesky LM, Insall RH (1998) Scar1 and the related Wiskott–Aldrich syndrome protein, WASP, regulate the actin cytoskeleton through the Arp2/3 complex. *Curr Biol* 8:1347–1356.
13. Orange JS, Stone KD, Turvey SE, Krzewski K (2004) The Wiskott–Aldrich syndrome. *Cell Mol Life Sci* 61:2361–2385.
14. Takenawa T, Suetsugu S (2007) The WASP-WAVE protein network: connecting the membrane to the cytoskeleton. *Nat Rev Mol Cell Biol* 8:37–48.
15. Ramesh N, Anton IM, Hartwig JH, Geha RS (1997) WIP, a protein associated with Wiskott–Aldrich syndrome protein, induces actin polymerization and redistribution in lymphoid cells. *Proc Natl Acad Sci USA* 94:14671–14676.
16. Martinez-Quiles N, *et al.* (2001) WIP regulates N-WASP-mediated actin polymerization and filopodium formation. *Nat Cell Biol* 3:484–491.
17. Kinley AW, *et al.* (2003) Cortactin interacts with WIP in regulating Arp2/3 activation and membrane protrusion. *Curr Biol* 13:384–393.
18. Krzewski K, Chen X, Orange JS, Strominger JL (2006) Formation of a WIP-, WASp-, actin-, and myosin IIA-containing multiprotein complex in activated NK cells and its alteration by KIR inhibitory signaling. *J Cell Biol* 173:121–132.
19. Anton IM, *et al.* (2003) WIP participates in actin reorganization and ruffle formation induced by PDGF. *J Cell Sci* 116:2443–2451.
20. Anton IM, *et al.* (2002) WIP deficiency reveals a differential role for WIP, the actin cytoskeleton in T, B cell activation. *Immunity* 16:193–204.
21. Kettner A, *et al.* (2004) WIP regulates signaling via the high affinity receptor for immunoglobulin E in mast cells. *J Exp Med* 199:357–368.
22. Peters PJ, *et al.* (1991) Cytotoxic T lymphocyte granules are secretory lysosomes, containing both perforin and granzymes. *J Exp Med* 173:1099–1109.
23. Gasman S, Chasserot-Golaz S, Malacombe M, Way M, Bader MF (2004) Regulated exocytosis in neuroendocrine cells: a role for subplasmalemmal Cdc42/N-WASP-induced actin filaments. *Mol Biol Cell* 15:520–531.
24. Merrifield CJ, Qualmann B, Kessels MM, Almers W (2004) Neural Wiskott Aldrich Syndrome Protein (N-WASP) and the Arp2/3 complex are recruited to sites of clathrin-mediated endocytosis in cultured fibroblasts. *Eur J Cell Biol* 83:13–18.
25. Takamori S, *et al.* (2006) Molecular anatomy of a trafficking organelle. *Cell* 127:831–846.
26. Orange JS, *et al.* (2003) The mature activating natural killer cell immunologic synapse is formed in distinct stages. *Proc Natl Acad Sci USA* 100:14151–14156.
27. Chen X, Trivedi PP, Ge B, Krzewski K, Strominger JL (2007) Many NK cell receptors activate ERK2 and JNK1 to trigger microtubule organizing center and granule polarization and cytotoxicity. *Proc Natl Acad Sci USA* 104:6329–6334.
28. de la Fuente MA, *et al.* (2007) WIP is a chaperone for Wiskott–Aldrich syndrome protein (WASP). *Proc Natl Acad Sci USA* 104:926–931.
29. Konno A, Kirby M, Anderson SA, Schwartzberg PL, Candotti F (2007) The expression of Wiskott–Aldrich syndrome protein (WASP) is dependent on WASP-interacting protein (WIP). *International immunology* 19:185–192.
30. Sims TN, *et al.* (2007) Opposing effects of PKCtheta and WASp on symmetry breaking and relocation of the immunological synapse. *Cell* 129:773–785.
31. Kaksonen M, Toret CP, Drubin DG (2006) Harnessing actin dynamics for clathrin-mediated endocytosis. *Nat Rev Mol Cell Biol* 7:404–414.
32. Naqvi SN, Zahn R, Mitchell DA, Stevenson BJ, Munn AL (1998) The WASp homologue Las17p functions with the WIP homologue End5p/verprolin and is essential for endocytosis in yeast. *Curr Biol* 8:959–962.
33. Efimov A, *et al.* (2007) Asymmetric CLASP-dependent nucleation of noncentrosomal microtubules at the trans-Golgi network. *Dev Cell* 12:917–930.
34. Stinchcombe JC, Majorovits E, Bossi G, Fuller S, Griffiths GM (2006) Centrosome polarization delivers secretory granules to the immunological synapse. *Nature* 443:462–465.
35. Stinchcombe JC, Bossi G, Booth S, Griffiths GM (2001) The immunological synapse of CTL contains a secretory domain and membrane bridges. *Immunity* 15:751–761.
36. Andzelm MM, Chen X, Krzewski K, Orange JS, Strominger JL (2007) Myosin IIA is required for cytolytic granule exocytosis in human NK cells. *J Exp Med* 204:2285–2291.
37. Kankaanpää P, Pahajoki K, Marjomäki V, Heino J, White D (2006) BioImageXD – New open source free software for the processing, analysis and visualization of multidimensional microscopic images. *Microsc Today* 14:12–16.
38. Costes SV, *et al.* (2004) Automatic and quantitative measurement of protein-protein colocalization in live cells. *Biophys J* 86:3993–4003.